Inorg. Chem. **2004**, *43*, 593–601

An ab Initio Study on Luminescent Properties and Aurophilic Attraction of Binuclear Gold(I) Complexes with Phosphinothioether Ligands

Qing-Jiang Pan and Hong-Xing Zhang*

State Key Laboratory of Theoretical and Computational Chemistry, Institute of Theoretical Chemistry, Jilin University, Changchun 130023, P. R. China

Received January 13, 2003

Electronic structures and spectroscopic properties of the binuclear head-to-tail $[Au_2(PH_2CH_2SH)_2]^{2+}$ (**1**) complex were investigated by ab initio calculations. The solvent effect of the complex in the acetonitrile solution was taken into account by the weakly solvated $[Au_2(PH_2CH_2SH)_2]^{2+}\cdot(MeCN)_2$ (**2**) moiety in the calculations. The ground-state geometries of **1** and **2** were fully optimized by the MP2 method, while their excited-state structures were optimized by the CIS method. Aurophilic attraction apparently exists between the two Au(I) atoms in the ground state and is strongly enhanced in the excited state. A high-energy phosphorescent emission was calculated at 337 nm for **1** in the absence of the interactions with solvent molecules and/or counteranion in solid state; however the lowest-energy emission of **2** was obtained at 614 nm with the nature of $^3A_u(s_\sigma) \rightarrow {}^1A_g(d_{\sigma^*})$ (metal-centered, MC) transition. The coordination of acetonitrile to the gold atom in solution results in a dramatic red shift of emission wavelength. The investigations on the head-to-tail $[Au_2(PH_2CH_2SCH_3)_2]^{2+}$ (**5**) and $[Au_2(PH_2CH_2SCH_3)_2]^{2+}\cdot(MeCN)_2$ (**6**) moieties indicate that the CH_3 substituent on the S atom causes blue shifts of emission wavelength for **5** and **6** with respect to **1** and **2**. By comparison between Au(I) thioether **1** and head-to-tail Au(I) thiolate $[Au_2(PH_2CH_2S)_2]$ (**7**), it is concluded that the S→Au dative bonding results in evidently different transition characteristics from the S–Au covalent bonding in the Au(I) thioether/thiolate complexes.

1. Introduction

The photoluminescence of Au(I) complexes as well as the relationship between the luminescent properties and aurophilic attraction of two Au(I) atoms has attracted a great deal of attention over the past three decades.[1−10] Many experimental and theoretical studies indicated that Au(I) complexes strongly luminesce, especially when the aurophilic attraction is present.[1,7−11] The energy of the interaction between the two Au(I) atoms has been estimated to be 7−15 kcal/mol, comparable to that of hydrogen bonds.[12−14] In the earlier theoretical studies, the SCF-X_α-SW method was applied to reveal the luminescent properties of the binuclear Au(I) phosphine complexes, and their lowest-energy emission was assigned as the transition localized on the Au(I) centers through analysis of the frontier orbitals of the ground state.[10] Recently, our investigation[11] on such Au(I) complexes using the second-order Møller−Plesset perturbation (MP2) and the single excitation configuration interaction (CIS) methods has indicated that the lowest-energy emission of the complexes in acetonitrile originates from $^3A_u(s_\sigma) \rightarrow {}^1A_g(d_{\sigma^*})$ (metal-centered, MC) transition. Moreover, the aurophilic attraction

* Corresponding author. Tel: (86)-431-8498966. Fax: (86)-431-8923907. E-mail: hxzhang@mail.jlu.edu.cn.

(1) (a) Rawashdeh-Omary, M. A.; Omary M. A.; Patterson, H. H.; Fackler, J. P., Jr. *J. Am. Chem. Soc.* **2001**, *123*, 11237. (b) van Zyl, W. E.; López-de-Luzuriaga, J. M.; Mohamed, A. A.; Staples, R. J.; Fackler, J. P., Jr. *Inorg. Chem.* **2002**, *41*, 4579. (c) van Zyl, W. E.; López-de-Luzuriaga, J. M.; Fackler, J. P., Jr. *J. Mol. Struct.* **2000**, *516*, 99.
(2) Bachman, R. E.; Bodolosky-Bettis, S. A.; Glennon, S. C.; Sirchio, S. A. *J. Am. Chem. Soc.* **2000**, *122*, 7146.
(3) Bardají, M.; Laguna, A.; Orera, V. M.; Villacampa, M. D. *Inorg. Chem.* **1998**, *37*, 5125.
(4) Yam, V. W. W.; Lo, K. K. W. *Chem. Soc. Rev.* **1999**, *28*, 323.
(5) Khan, Md. N. I.; King, C. Heinrich, D. D.; Fackler, J. P., Jr.; Porter, L. C. *Inorg. Chem.* **1989**, *28*, 2150.
(6) Narayanaswamy, R.; Young, M. A.; Parkhurst, E.; Ouellette, M.; Kerr, M. E.; Ho, K. M.; Elder, R. C. Bruce, A. E.; Bruce, M. R. M. *Inorg. Chem.* **1993**, *32*, 2506.
(7) Tang, S. S.; Chang, C. P.; Lin, I. J. B.; Liou, L. S.; Wang, J. C. *Inorg. Chem.* **1997**, *36*, 2294.
(8) Leung, K. H.; Phillips, D. L. Tse, M. C.; Che, C. M.; Miskowski V. M. *J. Am. Chem. Soc.* **1999**, *121*, 4799.
(9) Fernández, E. J.; Gimeno, C.; Laguna, A., et al. *J. Am. Chem. Soc.* **2000**, *122*, 7287.
(10) King, C.; Wang, J. C.; Khan, M. N. I.; Fackler, J. P., Jr. *Inorg. Chem.* **1989**, *28*, 2145.
(11) Zhang, H.-X.; Che, C.-M. *Chem. Eur. J.* **2001**, *7*, 4887.
(12) Pyykkö, P.; Mendizabal, F. *Inorg. Chem.* **1998**, *37*, 3018.
(13) Pathaneni, S. S.; Desiraju, G. R. *J. Chem. Soc., Dalton Trans.* **1993**, 319.
(14) Schmidbaur, H. *Gold Bull.* **1990**, *23*, 11.

10.1021/ic0300159 CCC: $27.50
Published on Web 12/18/2003

is dramatically strengthened in the $^3(d_{\sigma^*}s_\sigma)$ excited state, illustrating the relationship between the luminescent properties and Au^I-Au^I attraction in the complexes.

Au(I) complexes containing both phosphine and thiolate ligands have fascinating spectroscopic properties.[15−20] Like binuclear gold(I) phosphine complexes,[21−23] the phosphine gold(I) thiolates also have emissions with lifetimes in the microsecond range and large Stokes shifts in the visible region, and the emissions, in most cases, were experimentally attributed to Au → thiolate charge transfer (MLCT).[4−7,15−18] Bruce's studies on a series of binuclear phosphine Au(I) thiolates with or without Au^I-Au^I interaction showed that the Au^I-Au^I interaction is not a necessary condition for the luminescence and its presence does not significantly perturb the luminescence of the complexes.[15] However, Fackler and co-workers have investigated the luminescence in many mononuclear Au(phosphine)(thiolate) complexes and found the position of emission maximum can be affected by the presence of the intermolecular Au^I-Au^I interaction.[16] Very recently, the work of Eisenberg and co-workers on the luminescence of Au(I) dithiophosphate complexes has supported the assignment of Bruce and Fackler.[24] Eisenberg and co-workers pointed out that the charge transfer from ligand to metal should be elaborately divided into ligand to metal−metal charge transfer (LMMCT) and ligand to metal charge transfer (LMCT).[24] The former is clearly related to Au^I-Au^I interaction, but the latter is not.

In the complexes, the bonding nature of Au−S and Au−P is different because of the difference between S and P atoms in electronic structure. The phosphine always provides lone pair electrons to contribute to Au(I) atom to form the dative bond while the covalent bond is usually favored between Au and S atoms in most complexes. The $[Au_2(PPh_2CH_2SPh)_2]\cdot(CF_3SO_3)_2$ complex[25] is one of the rare examples of the Au(I) complexes containing the S→Au (gold−thioether) dative bonds instead of the Au−S (gold−thiolate) covalent bonds. Moreover, the synthetic pathway of the complex with S→Au dative bond is also different from the typical reaction between the gold precursor $[Au(tht)_2]CF_3SO_3$ (tht = tetrahydrothiophene) and phosphinothioether (PPh_2CH_2SPh) in the case of the gold derivatives.[6,10,15,19] The pathway for the Au(I) thioether complexes is that the phosphine first coordinates to the Au(I) atoms to form the $[AuCl(PPh_2CH_2SPh)]$ precursor and then two precursors dimerize to the desired product in the crystallization process. Such different synthetic pathways demonstrated that the thioether is a weaker Lewis base relative to phosphine, i.e., a weaker electron donor.

Since the presence of a bridging ligand facilitates the intramolecular interaction,[7,12] the gold(I) complex with the eight-membered ring conformation can serve as an ideal candidate for the investigation on the relationship between spectroscopic properties and aurophilicity.[1,11] In this paper, we employed ab initio methods to study the electronic structures and luminescent properties of the binuclear head-to-tail model $[Au_2(PH_2CH_2SH)_2]^{2+}$ (**1**) with the S→Au dative bonds and its weakly solvated moiety $[Au_2(PH_2CH_2SH)_2]^{2+}\cdot(MeCN)_2$ (**2**) as well as the solid-state model $[Au_2(PH_2CH_2SH)_2]\cdot(ClO)_2$. The results demonstrated that the lowest-energy phosphorescence either in acetonitrile or in the solid state has the nature of an MC transition, which clearly differs from the reported experimental assignment of MMLCT or MLCT for the binuclear phosphine Au(I) thiolates containing the Au−S covalent bonds.[6−7,15] The head-to-head isomers $[Au_2(PH_2CH_2SH)_2]^{2+}$ (**3**) and $[Au_2(PH_2CH_2SH)_2]^{2+}\cdot(MeCN)_2$ (**4**) also have the same transition properties as **1** and **2**. The head-to-tail $[Au_2(PH_2CH_2SCH_3)_2]^{2+}$ (**5**), $[Au_2(PH_2CH_2SCH_3)_2]^{2+}\cdot(MeCN)_2$ (**6**), and $[Au_2(PH_2CH_2SCH_3)_2]\cdot(ClO)_2$ moieties were taken into account to study the substituent effect on the sulfur atoms to the complexes. In addition, the comparison between **1** (thioether complex) and the head-to-tail $[Au_2(PH_2CH_2S)_2]$ (**7**) (thiolate complex) indicated that the S atoms contribute to the lowest-energy emission much more in the Au(I) thiolate complexes than in the Au(I) thioether complexes.

2. Computational Details and Theory

In the calculations, we used $[Au_2(PH_2CH_2SH)_2]^{2+}$ (**1**) as the computational model to represent the $[Au_2(PPh_2CH_2SPh)_2]^{2+}$ complex.[25] The similar model was applied in our previous work[11] by using dpm to replace dmpm, dppm, and dcpm for the $[Au_2(dmpm)_2]^{2+}$, $[Au_2(dppm)_2]^{2+}$, and $[Au_2(dcpm)_2]^{2+}$ complexes, respectively (dpm = bis(diphosphino)methane, dmpm = bis(dimethylphosphino)methane, dppm = bis(diphenylphosphino)methane, and dcpm = bis(dicyclohexylphosphino)methane). It is a general technique to employ hydrogen to substitute methyl, phenyl, etc. substituents in the ab initio study to save the computational resources. Häberlen and Rösch[26] have proved that the PH_3 provided a satisfactory model of the full PPh_3 or PMe_3 for the structural properties of the Au(I) complexes. Many authors[10,27−30] have successfully used such a model in their theoretical studies on related topics of Au(I) phosphine complexes. The model $[Au_2(PH_2CH_2SCH_3)_2]^{2+}$ (**5**) was calculated to certify the reasonability of using SH in the place of SCH_3 and SPh.

In this work, the C_i symmetry was adopted to settle the conformation of **1** and **5** in both the ground and excited states, which

(15) Jones, W. B.; Yuan, J.; Narayanaswamy, R.; Young, M. A.; Elder, R. C.; Bruce, A. E. Bruce, M. R. M. *Inorg. Chem.* **1995**, *34*, 1996.
(16) Forward, J. M.; Bohmann, D.; Fackler, J. P., Jr.; Staples, R. J. *Inorg. Chem.* **1995**, *34*, 6330.
(17) Hanna, S. D.; Zink, J. I. *Inorg. Chem.* **1996**, *35*, 297.
(18) Hanna, S. D.; Khan, S. I.; Zink, J. I. *Inorg. Chem.* **1996**, *35*, 5813.
(19) Bardají, M.; Laguna, A.; Vicente, J. *Inorg. Chem.* **2001**, *40*, 2675.
(20) Yam, V. W. W.; Cheng, E. C. C.; Zhou, Z. Y. *Angew. Chem., Int. Ed.* **2000**, *39*, 1683.
(21) Che, C. M.; Kwong, H. L.; Yam, V. W. W.; Cho, K. C. *J. Chem. Soc., Chem. Commun.* **1989**, 885.
(22) Fu, W. F.; Chan, K. C.; Miskowski, V. M.; Che, C. M. *Angew. Chem., Int. Ed.* **1999**, *38*, 2783.
(23) Jaw, H. R. C.; Savas, M.; Rogers, R. D.; Mason, W. R. *Inorg. Chem.* **1989**, *28*, 1028.
(24) Lee, Y. A.; McGarrah, J. E.; Lachicotte, R. J.; Eisenberg, R. *J. Am. Chem. Soc.* **2002**, *124*, 10662.
(25) Fernández, E. J.; López-de-Luzuraga, J. M.; Monge, M.; Rodríguez, M. A.; Crespo, O.; Gimeno, M. C.; Laguna, A.; Jones, P. G. *Inorg. Chem.* **1998**, *37*, 6002.
(26) Häberlen, O. D.; Rösch, N. *J. Phys. Chem.* **1993**, *97*, 4970.
(27) Schwerdtfeger, P.; Bruce, A. E.; Bruce, M. R. M. *J. Am. Chem. Soc.* **1998**, *120*, 6587.
(28) Fernández, E. J.; Gimeno, M. C.; Jones, P. G.; Laguna, A.; Laguna, M.; López-de-Luzuriaga, J. M.; Rodriguez, M. A. *Chem. Ber.* **1995**, *128*, 121.
(29) Dunlap, B. I.; Rösch, N. *Adv. Quantum Chem.* **1990**, *21*, 317.
(30) Dunlap, B. I.; Connolly, J. W.; Sabin, J. R. *J. Chem. Phys.* **1979**, *71*, 3396.

is consistent with the data of X-ray crystal diffraction of $[Au_2(PPh_2CH_2SPh)_2]^{2+}$.[25] Because the solvent effect strongly affects the luminescence of the Au(I) complexes according to experimental and theoretical studies,[10,11,17,18,21−23] we employed the similar solvated model of our previous work[11] to account for the electronic structures and spectroscopic properties of **1** and **5** in the acetonitrile solution, namely, the acetonitrile molecule coordinates to the Au(I) atom in **1** and **5** to form quasi three-coordinated $[Au_2(PH_2CH_2SH)_2]^{2+}\cdot(MeCN)_2$ (**2**) and $[Au_2(PH_2CH_2SCH_3)_2]^{2+}\cdot(MeCN)_2$ (**6**) moieties.

The ground- and excited-state structures of **1**−**6** were fully optimized using the MP2 and CIS methods (considering electron correlation effects), respectively. In the calculations, quasi-relativistic pseudopotentials of the Au, S, and P atoms proposed by Hay and Wadt[31] with 19, 6, and 5 valence electrons respectively were employed and the LANL2DZ basis sets associated with the pseudopotential were adopted. To describe precisely the metallophilic attraction and the molecular properties, one additional f-type function was implemented for Au ($\alpha_f = 0.2$) and one d-type function was added to S ($\alpha_d = 0.421$) and to P ($\alpha_d = 0.34$), respectively.[12] The basis sets were taken as Au(8s6p3d1f/3s3p2d1f), S(3s3p1d/2s2p1d), P(3s3p1d/2s2p1d), N(10s5p/3s2p), C(10s5p/3s2p), and H(4s/2s). Thus, 148 basis functions and 80 electrons for **1** and **3**, 214 basis functions and 124 electrons for **2** and **4**, 174 basis functions and 96 electrons for **5**, and 240 basis functions and 140 electrons for **6** were included in the calculations. All the calculations were accomplished by using the *Gaussian98* program package[32] on an Origin/3800 server.

3. Result and Discussion

3.1. The Ground-State Geometries for $[Au_2(PH_2CH_2SH)_2]^{2+}$ and $[Au_2(PH_2CH_2SH)_2]^{2+}\cdot(MeCN)_2$. The full MP2 optimizations on head-to-tail $[Au_2(PH_2CH_2SH)_2]^{2+}$ (**1**) and its solvated model $[Au_2(PH_2CH_2SH)_2]^{2+}\cdot(MeCN)_2$ (**2**) indicated that **1** and **2** both bear ^1A_g ground states. Their structures are depicted in Figure 1, and the main optimized geometry parameters are listed in Table 1 together with the X-ray crystal diffraction data of $[Au_2(PPh_2CH_2SPh)_2]\cdot(CF_3SO_3)_2$.[25] As shown in Figure 1a, the two phosphinothioether ligands, PH_2CH_2SH, adopt trans-coordination to the two Au(I) atoms, presenting a head-to-tail isomer. In complex **1**, the Au(I) takes a nearly linear two-coordinated geometry with the P−Au−S angle of 174.9°, comparable to the experimental 175.1° as seen in Table 1. The calculated 177.0° dihedral angle of P−Au−Au−S shows that the $Au_2P_2S_2$ unit is nearly coplanar. However, the weak interaction between Au(I) atom and acetonitrile in **2** results in the $Au_2P_2S_2$ distortion from the plane, which is reflected by the calculated

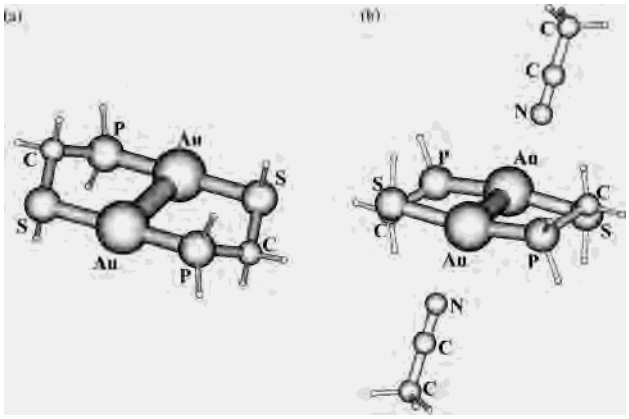

Figure 1. The optimized ^1A_g ground-state structures by the MP2 method for (a) $[Au_2(PH_2CH_2SH)_2]^{2+}$ (**1**) and (b) $[Au_2(PH_2CH_2SH)_2]^{2+}\cdot(MeCN)_2$ (**2**).

P−Au−Au−S dihedral angle of 168.4°. The calculated Au−Au, Au−P, and Au−S distances for **1** are 2.979, 2.341, and 2.424 Å, respectively, which correspond to 2.902, 2.272, and 2.362 Å for $[Au_2(PPh_2CH_2SPh)_2]\cdot(CF_3SO_3)_2$ in the experiment.[25] The electronegativity of the S atom is stronger than that of the P atom, and the two atoms have nearly identical atomic radii, so the about 0.1 Å longer distance of Au−S than Au−P either in **1** or in **2** illustrates that phosphine is a better electron donor than thioether in the $[Au_2(PH_2CH_2SH)_2]^{2+}$ complex. In fact, in the synthetic process of the $[Au_2(PPh_2CH_2SPh)_2]\cdot(CF_3SO_3)_2$ complex, the $[AuCl(PPh_2CH_2SPh)]$ precursor presents the P→Au dative bond, but not the S→Au dative bond.[25]

The calculated Au^I-Au^I separations of 2.979 and 2.953 Å of the ground states for **1** and **2**, respectively, are much less than the van der Waals contact of 3.4 Å,[33] implying significant aurophilic attraction between the two Au(I) atoms. The natural bond orbital (NBO) analysis from the MP2 calculations on **1** showed that the Au atom has a net +0.45 electronic charge, while electronic charges residing on the P atom and S atom are +0.46 and +0.08, respectively, indicating that the electrons of the S and P atoms transfer to the original 6s and 6p empty orbitals of Au(I). Consequently, the closed-shell electronic configuration, $5d^{10}6s^0$, is no longer kept in $[Au_2(PH_2CH_2SH)_2]^{2+}$ but $5d^{9.83}6s^{0.71}6p^{0.01}$ instead. Such a destruction of Au closed-shell structure may be one of the predominant driving forces to cause aurophilic attraction.

As shown in Figure 1b, the optimized structure of the ground state of **2** resembles the X-ray crystal structures of $[Au_2(dppm)_2]X_2$ (X = Cl, Br, and BH_3CN).[5,34] In $[Au_2(dppm)_2]Cl_2$, for example, the two chloro anions lie up and down the Au_2P_4 plane in the opposite direction, forming the Cl−Au−Au angle of 97° just like our calculated N−Au−Au angle of 104.0° as given in Table 1. In addition, the structure of **2** is in agreement with that of $[Au_2(PH_2CH_2PH_2)_2]^{2+}\cdot(MeCN)_2$ in the previous study.[11]

(31) (a) Wadt, W. R.; Hay, P. J. *J. Chem. Phys.* **1985**, *82*, 284. (b) Hay, P. J.; Wadt, W. R. *J. Chem. Phys.* **1985**, *82*, 299.
(32) Frisch, M. J.; Trucks, G. W.; Schlegel, H. B.; Scuseria, G. E.; Robb, M. A.; Cheeseman, J. R.; Zakrzewski, V. G.; Montgomery, J. A., Jr.; Stratmann, R. E.; Burant, J. C.; Dapprich, S.; Millam, J. M.; Daniels, A. D.; Kudin, K. N.; Strain, M. C.; Farkas, O.; Tomasi, J.; Barone, V.; Cossi, M.; Cammi, R.; Mennucci, B.; Pomelli, C.; Adamo, C.; Clifford, S.; Ochterski, J.; Petersson, G. A.; Ayala, P. Y.; Cui, Q.; Morokuma, K.; Malick, D. K.; Rabuck, A. D.; Raghavachari, K.; Foresman, J. B.; Cioslowski, J.; Ortiz, J. V.; Baboul, A. G.; Stefanov, B. B.; Liu, G.; Liashenko, A.; Piskorz, P.; Komaromi, I.; Gomperts, R.; Martin, R. L.; Fox, D. J.; Keith, T.; Al-Laham, M. A.; Peng, C. Y.; Nanayakkara, A.; Challacombe, M.; Gill, P. M. W.; Johnson, B.; Chen, W.; Wong, M. W.; Andres, J. L.; Gonzalez, C.; Head-Gordon, M.; Replogle, E. S.; Pople, J. A. *Gaussian 98*, revision A.9; Gaussian, Inc.: Pittsburgh, PA, 1998.
(33) Bondi, A. *J. Phys. Chem.* **1964**, *68*, 441.
(34) (a) Schmidbaur, H.; Wohlleben, A.; Schuber, U.; Frank, A.; Huttner, G. *Chem. Ber.* **1977**, *110*, 2751−2757. (b) Shain, J.; Fackler, J. P., Jr. *Inorg. Chim. Acta* **1987**, *131*, 157−158. (c) Kozelka, J.; Oswald, H. R.; Dubler, E. *Acta Crystallogr.* **1986**, *C42*, 1007.

Table 1. The Optimized Main Geometry Parameters of the Ground State and the Triplet Excited State for Head-to-Tail $[Au_2(PH_2CH_2SH)_2]^{2+}$ (**1**), Head-to-Tail $[Au_2(PH_2CH_2SH)_2]^{2+}\cdot(MeCN)_2$ (**2**), Head-to-Head $[Au_2(PH_2CH_2SH)_2]^{2+}$ (**3**), Head-to-Head $[Au_2(PH_2CH_2SH)_2]^{2+}\cdot(MeCN)_2$ (**4**), Head-to-Tail $[Au_2(PH_2CH_2SCH_3)_2]^{2+}$ (**5**), and Head-to-Tail $[Au_2(PH_2CH_2SCH_3)_2]^{2+}\cdot(MeCN)_2$ (**6**) Using the MP2 and CIS Methods Respectively

	1		**2**		**3**		***4***[a]		**5**		**6**		
params	^1A_g	^3A_u	^1A_g	^3A_u	^1A	^3A	^1A	^3A	^1A_g	^3A_u	^1A_g	^3A_u	exptl[b]
						Bond Length (Å)							
Au−Au	2.979	2.715	2.953	2.657	2.972	2.994	2.996	2.730	2.975	2.710	2.919	2.664	2.902
Au−P	2.341	2.558	2.318	2.623	2.372	2.435	2.370	2.556	2.342	2.555	2.325	2.631	2.272
Au−S	2.424	2.705	2.449	2.981	2.396	2.894	2.427	2.892	2.406	2.641	2.422	2.890	2.362
P···S	3.160	3.154	3.132	3.078	3.160	3.129	3.124	3.091	3.164	3.169	3.111	3.079	
Au−N			2.567	2.336			2.587	2.441			2.898	2.361	
						Bond Angle (deg)							
P−Au−S	174.9	170.1	167.9	169.8					175.4	169.1	174.5	169.6	175.1
P−Au−P					175.9	178.8	166.0	176.6					
S−Au−S					168.7	178.5	170.9	171.2					
P−Au−Au	87.1	94.5	89.0	94.8	88.0	90.6	83.0	91.7	87.4	94.1	87.4	93.5	91.4
S−Au−Au	97.0	94.9	94.2	93.1	95.7	90.7	94.5	94.4	97.0	95.8	96.9	94.6	93.5
N−Au−Au			104.0	174.3			180.0	180.0			108.3	176.3	
						Dihedral Angle (deg)							
P−Au−Au−S	177.0	177.0	168.4	173.6	168.5	169.4	151.9	168.8	178.8	175.6	176.6	173.4	
C−P−S−Au	136.3	136.7	126.4	141.0	131.2	133.0	129.9	134.2	135.5	139.9	136.8	141.6	

[a] **3** has C_2 symmetry, and **4** belongs to the C_1 point group. [b] The X-ray crystal diffraction data of the $[Au_2(PPh_2CH_2SPh)_2]\cdot(CF_3SO_3)_2$ complex from ref 25.

Table 2. The Calculated Absorption, Fluorescence, and Phosphorescence Wavelengths and Their Transition Nature of $[Au_2(PH_2CH_2SH)_2]^{2+}\cdot(MeCN)_2$ (**2**), Together with Oscillator Strength for the Absorptions and Fluorescence

	transition nature	wavelength (nm)	oscillator strength
absorption	$X^1A_g \rightarrow A^1A_u$	220	0.256
	$X^1A_g \rightarrow B^1A_u$	177	0.011
	$X^1A_g \rightarrow C^1A_u$	174	0.164
fluorescence	$^1A_u \rightarrow {}^1A_g$	380	0.126
phosphorescence	$^3A_u \rightarrow {}^1A_g$	614	

3.2. The Absorption Spectra for $[Au_2(PH_2CH_2SH)_2]^{2+}\cdot(MeCN)_2$. According to the vertical electron transition mechanism in the absorption process, the optimized ground-state geometry of **2** was kept, while the CIS calculations were performed to calculate the excited states related to the absorption. We obtained three dipole-allowed transitions of **2** that represent the possible absorptions of $[Au_2(PH_2CH_2SH)_2]^{2+}$ in acetonitrile. The wavelengths of these absorptions were presented in Table 2, together with their corresponding oscillator strengths and transition characters.

With respect to the ^1A_g ground state under the C_i point group, the $^1A_g \rightarrow {}^1A_u$ transition is dipole-allowed. We calculated three low-lying ^1A_u excited states and list their natural atomic orbital populations for **2** together with that of the ^1A_g ground state in Table 3.

The calculated lowest-energy absorption of **2** is at 220 nm with the largest oscillator strength of 0.256, which may be most likely to be observed in experiment. We can see from Table 3 that the transition localized on the gold centers plays a main role in the $X^1A_g \rightarrow A^1A_u$ transition, while the population on the phosphinothioether (PH_2CH_2SH) ligand and the MeCN molecule in the transition process is almost unchanged. The electronic configurations of Au(I) atoms in the X^1A_g ground state and the A^1A_u excited state are $4f^{0.003}5d^{9.834}6s^{0.619}6p^{0.017}$ and $4f^{0.005}5d^{9.618}6s^{0.620}6p^{0.185}$, respectively. In the transition, the 5d orbital of the Au atom loses about 0.22 electron that transfers to the Au 6p orbital. So we assigned the 220 nm absorption as the $d_{\sigma^*} \rightarrow p_\sigma$ (MC) transition with the nature of $X^1A_g \rightarrow A^1A_u$, which agrees with the assignment of the lowest-energy absorption for the binuclear Au(I) phosphine complexes in experiment and theory.[10,11,21,22] The density diagrams of the frontier orbitals for the $X^1A_g \rightarrow A^1A_u$ transition shown in Figure 2 can intuitively illustrate that significant electron transition occurs around the Au(I) centers. The configuration arising from the electron excitation, $31a_u \rightarrow 32a_g$, has the largest coefficient of 0.645 in the CI wave functions, where the electron density focuses on each Au atom to form d_{σ^*} antibonding orbitals in $31a_u$ (HOMO), but in $32a_g$ (LUMO) the electron density mainly localizes between the two Au atoms to form a p_σ bonding orbital.

For the B^1A_u excited state of **2**, the charge transfer mainly takes place in the $[Au_2(PH_2CH_2SH)_2]^{2+}$ part as shown in

Table 3. The Natural Atomic Orbital Populations for the ^1A_g Ground State and Three Low-Lying ^1A_u Excited States for $[Au_2(PH_2CH_2SH)_2]^{2+}\cdot(MeCN)_2$ (**2**) Calculated by the CIS Method

atom	orbitals	X^1A_g	A^1A_u	B^1A_u	C^1A_u
Au	6s	0.619	0.620	0.676	0.658
	6p	0.017	0.185	0.062	0.103
	5d	9.834	9.618	9.710	9.699
	4f	0.003	0.005	0.004	0.004
P	3s	1.333	1.325	1.347	1.334
	3p	3.142	3.184	3.143	3.144
	3d	0.061	0.063	0.061	0.062
S	3s	1.658	1.657	1.668	1.660
	3p	4.230	4.204	4.110	4.155
	3d	0.042	0.042	0.050	0.046
C1	2s	1.220	1.244	1.248	1.245
	2p	3.586	3.593	3.642	3.613
H_{C1}	1s	0.721	0.721	0.717	0.717
$H_{C1'}$	1s	0.720	0.720	0.720	0.720
H_{P1}	1s	0.999	1.001	1.002	0.998
$H_{P1'}$	1s	0.978	0.983	0.978	0.981
H_S	1s	0.849	0.851	0.882	0.878
N	2s	1.610	1.607	1.606	1.609
	2p	4.028	4.028	4.027	4.007
C2	2s	0.918	0.917	0.917	0.919
	2p	2.554	2.552	2.553	2.568
C3	2s	1.140	1.140	1.140	1.140
	2p	3.549	3.548	3.549	3.548
H_{C3}	1s	0.732	0.732	0.732	0.732

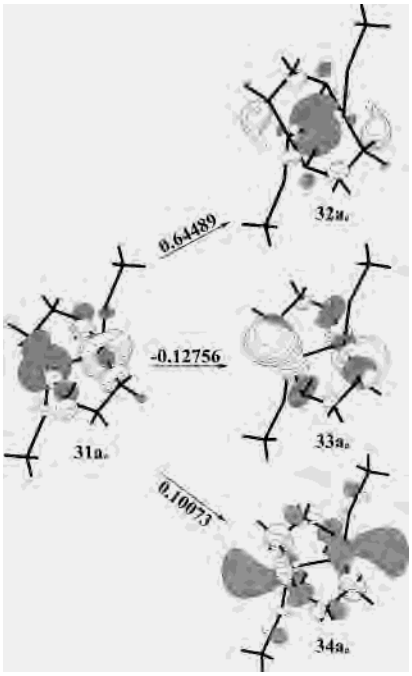

Figure 2. The single electron transitions with |CI coefficient| > 0.1 in the CIS calculations for the 220 nm $X^1A_g \rightarrow A^1A_u$ absorption of $[Au_2(PH_2CH_2SH)_2]^{2+}\cdot(MeCN)_2$ (**2**).

Table 3, while the population on the MeCN molecules remains constant. There is about 0.12 electron to transfer from the 5d orbital of Au atom to the 6s and 6p orbitals at the ratio 1:1 statistically in the absorption process. In addition, there is some charge transfer between the sulfur and carbon atoms inside the PH_2CH_2SH ligand. So the 177 nm absorption arising from $X^1A_g \rightarrow B^1A_u$ was attributed to $d_{\sigma^*} \rightarrow (sp)_\sigma$ mixed with some intraligand transition in the phosphinothioether ligand, where $(sp)_\sigma$ means a σ bonding orbital with a mixed s and p orbital character. The third absorption was calculated at 174 nm with the nature of $X^1A_g \rightarrow C^1A_u$ transition. As shown in Table 3, all the population in the whole molecule changes. By analyzing the natural atomic orbital population and the wave functions, the transition was assigned to the combination of $d_{\sigma^*} \rightarrow (sp)_\sigma$, intra-phosphinothioether transtion and $\pi \rightarrow \pi^*$ in MeCN. Since this absorption band is clearly related to the solvent, its wavelength is expected to change with different solution in experiment.

In the CIS calculations on **2**, the triplet excited states related to the spin-forbidden absorptions were also considered. As a heavy metal element, the spin−orbit coupling of the Au atom should be large, thus the singlet-to-triplet transition may appear as weak tails in the absorption spectra. The lowest-energy absorption from the $X^1A_g \rightarrow {}^3A_u$ transition was calculated at 260 nm, which belongs to $d_{\sigma^*} \rightarrow p_\sigma$ (MC) transition, the same transition character as the dipole- and spin-allowed $X^1A_g \rightarrow A^1A_u$ transition of 220 nm.

3.3. The Excited-State Geometries for $[Au_2(PH_2CH_2SH)_2]^{2+}$ and $[Au_2(PH_2CH_2SH)_2]^{2+}\cdot(MeCN)_2$. To describe the emissive properties of complexes **1** and **2**, the CIS method was used to optimize geometries of the excited states for the complexes. Their structures are shown in Figure 3, and the main calculated geometry parameters are listed in Table 1.

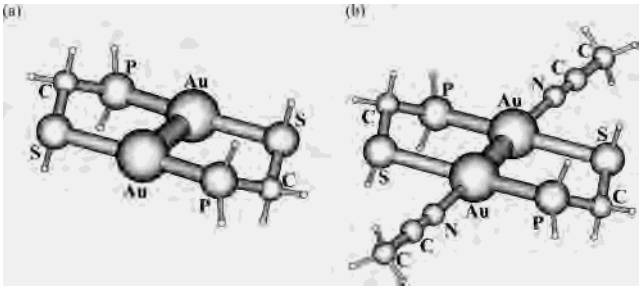

Figure 3. The optimized ^3A_u excited-state structures by the CIS method for (a) $[Au_2(PH_2CH_2SH)_2]^{2+}$ (**1**) and (b) $[Au_2(PH_2CH_2SH)_2]^{2+}\cdot(MeCN)_2$ (**2**).

With respect to the ^3A_u excited states of **1** and **2**, the geometry structures have the following two major changes compared with those of their corresponding ^1A_g ground states as shown in Table 1. First, the Au^I-Au^I separations are greatly shortened from 2.979 and 2.953 Å to 2.715 and 2.657 Å for **1** and **2**, respectively, while the distances of Au−P and Au−S are strongly elongated, which indicates that the bonding interaction between the two Au(I) atoms weakens the S→Au and P→Au bonds. Second, the N−Au−Au angle changes from 104.0° in the ^1A_g ground state to 174.3° in the ^3A_u excited state for **2**. The interaction between the Au(I) atom and the N atom in MeCN is greatly enhanced, for the Au−N distance of the ^3A_u excited state is about 0.23 Å shorter than that of the ^1A_g ground state.

In addition, there are apparent differences between pure cation **1** and its solvated model **2** in geometry of the ^3A_u excited state as shown in Table 1. The solvation of acetonitrile makes the Au^I-Au^I distance shorter, but the Au−P and Au−S bond lengths longer, especially the Au−S distance. This implies that the coordination of N atom to Au atom slightly strengthens Au^I-Au^I aurophilic attraction and also competes with the coordination of P→Au and S→Au.

In the ^3A_u excited state of **2**, the planar conformation between the $Au_2P_2S_2$ plane and the two MeCN molecules is favored as shown in Figure 3b, similar to those of d^9-d^9 metal complexes $[Au_2Y_2(CH_2PPh_2CH_2)_2]$ (Y = Cl, Br, I, and NO_2)[35] that contain very short Au−Au distances (about 2.63 Å). Thus, we conjecture that there is the formation of an Au−Au single bond in the excited state of **2** just like that in the d^9-d^9 complexes.

3.4. The Emission spectra for $[Au_2(PH_2CH_2SH)_2]^{2+}$ and $[Au_2(PH_2CH_2SH)_2]^{2+}\cdot(MeCN)_2$. In the CIS calculations, the lowest-energy emission for **2** was obtained at 614 nm originating from the $^3A_u \rightarrow {}^1A_g$ transition. We present the natural atomic orbital population of the excited state and its

(35) (a) Trzcinska-Bancroft, B.; Khan, Md. N. I.; Fackler, J. P., Jr. *Organometallics* **1988**, *7*, 993. (b) Mazany, A. M.; Fackler, J. P., Jr. *J. Am. Chem. Soc.* **1984**, *106*, 801. (c) Basil, J. D.; Murray, H. H.; Fackler, J. P., Jr.; Tocher, J.; Mazany, A. M.; Trzcinska-Bancroft, B.; Knachel, H.; Dudis, D.; Delord, T. J.; Marlerl, D. O. *J. Am. Chem. Soc.* **1985**, *107*, 6908. (d) Carlson, T. F.; Fackler, J. P., Jr. *J. Organomet. Chem.* **2000**, *596*, 237.

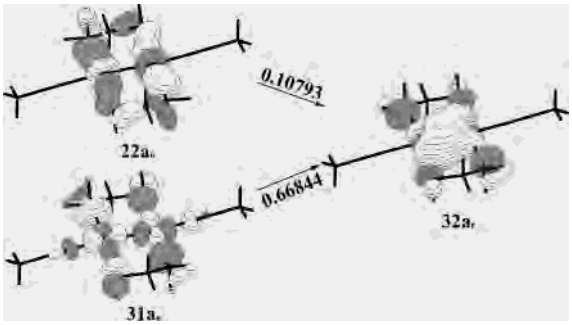

Figure 4. The single electron transitions with |CI coefficient| > 0.1 in the CIS calculations for the 614 nm $^3A_u \rightarrow {}^1A_g$ phosphorescence of $[Au_2(PH_2CH_2SH)_2]^{2+}\cdot(MeCN)_2$ (**2**).

Table 4. The Natural Atomic Orbital Populations for the ^3A_u Excited State and the Corresponding ^1A_g Ground State for $[Au_2(PH_2CH_2SH)_2]^{2+}\cdot(MeCN)_2$ (**2**) Involved in the 614 nm Phosphorescence

atoms	orbitals	^1A_g	^3A_u	atoms	orbitals	^1A_g	^3A_u
Au	6s	0.467	0.769	H_{C1}	1s	0.729	0.731
	6p	0.018	0.037	$H_{C1'}$	1s	0.733	0.733
	5d	9.894	9.518	H_{P1}	1s	1.008	1.008
	4f	0.002	0.003	$H_{P1'}$	1s	0.991	0.995
P	3s	1.363	1.388	H_S	1s	0.861	0.865
	3p	3.139	3.194	N	2s	1.562	1.564
	3d	0.052	0.052		2p	4.068	4.068
S	3s	1.666	1.668	C2	2s	0.888	0.888
	3p	4.260	4.221		2p	2.570	2.569
	3d	0.035	0.035	C3	2s	1.124	1.124
C1	2s	1.203	1.204		2p	3.552	3.552
	2p	3.608	3.607	H_{C3}	1s	0.735	0.735

corresponding ground state in Table 4. In the transition, the population of Au atoms changes greatly, while the population of other atoms in **2** is almost kept unchanged. The electronic configuration of the Au atom is $4f^{0.002}5d^{9.894}6s^{0.467}6p^{0.018}$ and $4f^{0.003}5d^{9.518}6s^{0.769}6p^{0.037}$ for the ^1A_g ground state and the ^3A_u excited state, respectively. In the emissive process, there is about 0.30 electron to transfer from the 6s orbital of Au atom to the 5d orbital. Thus, the 614 nm phosphorescence is clearly the $s_\sigma \rightarrow d_{\sigma^*}$ (MC) transition. The density diagrams of the frontier orbitals for the transition are depicted in Figure 4, which can help us intuitively understand the $^3A_u(s_\sigma) \rightarrow {}^1A_g(d_{\sigma^*})$ transition process. The electron density focusing around the P and S atoms in the main electron excitation, $31a_u \rightarrow 32a_g$, is nearly unchanged while the Au atomic orbital characters are apparently different. This illustrates that the electron transition mainly occurs inside Au centers. In $31a_u$ (HOMO) the electron occupies the $5d_{\sigma^*}$ antibonding orbitals, but in $32a_g$ (LUMO) the electron resides in the 6s orbital to result in the formation of a Au−Au σ single bond. The analysis about electron density distribution also explains why the Au^I-Au^I attraction is strongly enhanced in the excited state.

In phosphine Au(I) thiolates, the electron-rich phosphine ligand usually provides lone pair electrons and the dative bond from the P to Au(I) atoms is preferred, while the thiolate ligand, an anion, favors the Au−S covalent bond. In such complexes, the lowest-energy emission has Au−Au → thiolate (MMLCT) or Au → thiolate (MLCT) transitions in nature. The thiolate ligands are greatly involved in the transition, but the phosphine ligands play only a little role.

Table 5. The Natural Atomic Orbital Populations for the ^1A_g Ground State and the ^3A_u Excited State for $[Au_2(PH_2CH_2SH)_2]^{2+}$ (**1**) Involved in the 337 nm Phosphorescence

atoms	orbitals	^1A_g	^3A_u	atoms	orbitals	^1A_g	^3A_u
Au	6s	0.601	0.777	C1	2s	1.207	1.213
	6p	0.017	0.075		2p	3.601	3.602
	5d	9.876	9.626	H_{C1}	1s	0.718	0.719
	4f	0.003	0.004	$H_{C1'}$	1s	0.723	0.723
P	3s	1.344	1.349	H_{P1}	1s	0.985	0.988
	3p	3.140	3.132	$H_{P1'}$	1s	0.960	0.969
	3d	0.057	0.056	H_S	1s	0.838	0.840
S	3s	1.660	1.663				
	3p	4.232	4.226				
	3d	0.040	0.039				

However, the $[Au_2(PH_2CH_2SH)_2]^{2+}$ complex belongs to one of a few examples of Au(I) complexes with the S→Au dative bond, which is similar to the bonding nature of the bridging phosphine complex, $[Au_2(PH_2CH_2PH_2)_2]^{2+}$. So its MC luminescent properties for the 614 nm phosphorescence are similar to the 557 nm emission of $[Au_2(PH_2CH_2PH_2)_2]^{2+}$, but different from the reported assignment (MMLCT or MLCT) for most phosphine Au(I) thiolates.[6−7,15−18]

For the ^1A_u excited state of **2**, the geometry was fully optimized under the CIS calculations, and the 380 nm $^1A_u \rightarrow {}^1A_g$ fluorescence with an oscillator strength of 0.126 was obtained as shown in Table 2. The Au^I-Au^I distance is 2.731 Å for the state. By analyzing the wave functions of the ^1A_u excited state and its corresponding ^1A_g ground state, the transition was also assigned to MC transition in nature. For complexes $[Au_2(P\text{-}P)(S\text{-}S)]$ (P-P = dmpm, dppm and S-S = i-mnt, dtc; i-mnt = $S_2C_2(CN)_2^{2-}$, dtc = $S_2CNEt_2^-$),[7] the 400 nm emission was observed in lower-concentration acetonitrile solution at room temperature and was attributed to MC transition from the singlet excited state to the ground state in experiment, in consistence with our calculated 380 nm $^1A_u \rightarrow {}^1A_g$ emission.

For **1** without solvation, a 337 nm emission of the $^3A_u \rightarrow {}^1A_g$ transition was obtained under the CIS calculations, and its natural atomic orbital populations for the ^3A_u excited state and the corresponding ^1A_g ground state are listed in Table 5, which shows that the transition is metal-localized. The electronic configuration of the Au atom is $4f^{0.003}5d^{9.876}6s^{0.601}6p^{0.017}$ for the ^1A_g state and $4f^{0.004}5d^{9.626}6s^{0.777}6p^{0.075}$ for the ^3A_u state. The Au 5d orbital gets a total of 0.25 electron from 6s (0.18) and 6p (0.06) orbitals in the transition, so the emission of 337 nm was attributed to the $^3A_u((sp)_\sigma) \rightarrow {}^1A_g(d_{\sigma^*})$ transition, in which the $(sp)_\sigma$ bonding has 75% s character and 25% p character. In the previous study,[11] we have proved that the weak interaction between the $[Au_2(dpm)_2]^{2+}$ cation and its counteranion results in a red shift of the lowest-energy emission in the solid state and, moreover, the interaction is electrostatic in nature. Herein, we used the ClO^- anion to replace the $[CF_3SO_3]^-$ counteranion to save the computational resources, considering the electrostatic interaction between the cation and the anion. In the calculations, the anions and two Au atoms were kept collinear. The distance of R(Au−OCl) changes from 10 to 3 Å, and the corresponding emission varies from 339 nm to 396 nm. The counteranion added into **1** results in the red shift of the emission wavelength in the solid state. It has

been reported that $R(Au-OSO_2CF_3)$ is 3.093 Å in a crystal of $[Au_2(PPh_2CH_2SPh)_2]\cdot[CF_3SO_3]_2$,[25] thus, the solid-state emission of **1** was expected at 400 nm around.

To understand further the relationship between the aurophilic attraction and phosphorescence in **1**, the reference molecule, $[PH_3AuSH_2]^+$ (**8**), was taken into account. By employing the same method and basis sets as those for **1**, the calculation presented for **8** a 247 nm lowest-energy phosphorescent emission with an (sp) → d transition inside the Au atom, which corresponds to the 337 nm phosphorescent emission arising from the $(sp)_\sigma \rightarrow d_{\sigma^*}$ transition between the two Au(I) atoms for **1**. The aurophilic attraction combines the (sp) → d transition of **8** into the $(sp)_\sigma \rightarrow d_{\sigma^*}$ transition of **1**, and the emission wavelength red-shifts by about 90 nm from 247 to 337 nm. Bruce and co-workers[27] have studied the relationship between the Au^I-Au^I aurophilicity and the excited states for the *cis*- and *trans*-$X_2Au_2C_2H_2(PH_2)_2$ (X = Cl, Br, and I) using ab initio methods. Their calculations indicated that the aurophilic interaction causes a stabilization of the first singlet excited state in the cis-complex. The aurohilicity leads to a red shift in the spectrum of the cis isomers relative to the trans isomers.

Apparently, the lowest-energy phosphorescent emission of $[Au_2(PH_2CH_2SH)_2]^{2+}$ in solution (614 nm) has a large red shift to that in gas phase (337 nm). The coordination of acetonitrile to Au(I) atom in the ^3A_u excited state of **2** results in the stronger Au^I-Au^I aurophilicity in the solution (2.657 Å) than that in gas phase (2.715 Å), which should be responsible for the shift. Moreover, Au 6s character in the LUMO of **2** is nearly 100%, while that of **1** is just 75%. It is well established that the 6s orbital energy is lower than 6p's. The more s orbital participation stabilizes the LUMO orbital and further reduces the emission energy. Therefore, the red shift from the 337 nm in gas phase to the 614 nm in solution for complex **1** was attributed to the coordination effect and the reinforcement of Au^I-Au^I aurophilicity.

3.5. The Head-to-Head $[Au_2(PH_2CH_2SH)_2]^{2+}$ and $[Au_2(PH_2CH_2SH)_2]^{2+}\cdot(MeCN)_2$ Isomers. Using the same methods and basis sets as employed for **1** and **2**, head-to-head $[Au_2(PH_2CH_2SH)_2]^{2+}$ (**3**) and its solvated model $[Au_2(PH_2CH_2SH)_2]^{2+}\cdot(MeCN)_2$ (**4**) were investigated. As isomers of **1** and **2**, complexes **3** and **4** have the C_2 and C_1 symmetries, respectively.

The calculated ground- and excited-state geometry parameters are listed in Table 1, and the corresponding optimized structures are shown in S-Figure I (Supporting Information). Most of such optimized parameters of **3** and **4** are in agreement with those of **1** and **2**, respectively. The lowest-energy phosphorescent emissions of **3** and **4** were obtained at 383 and 473 nm, respectively. By analyzing the change of the natural atomic orbital populations in the transitions as shown in S-Table 1 (Supporting Information), both the emissions have MC transition character, just like the $^3A_u \rightarrow {}^1A_g$ emissions of **1** and **2**.

By comparison of the MP2 energy of the ground states between **1** and **3** (see S-Table 2, Supporting Information), it was concluded that the head-to-tail isomer is relatively stable. In fact, head-to-tail $[Au_2(PPh_2CH_2SPh)_2]\cdot(CF_3SO_3)_2$ has been synthesized in the experiment,[25] but no head-to-head isomer was reported.

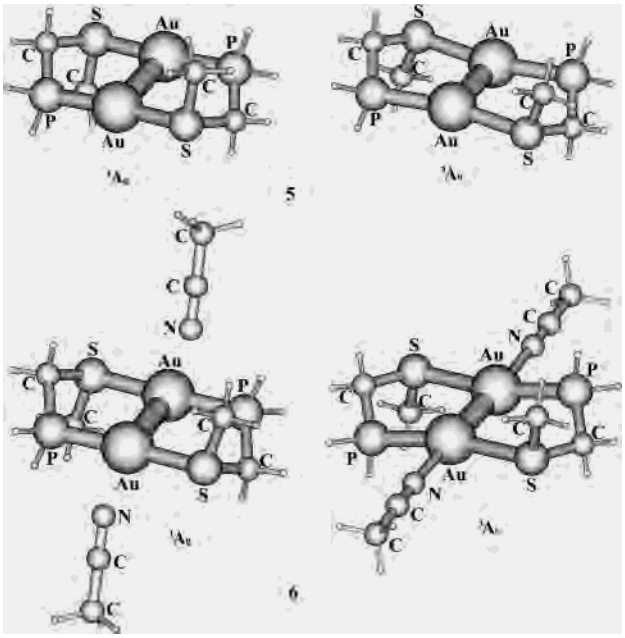

Figure 5. The optimized structures of the ^1A_g ground and the ^3A_u excited states for $[Au_2(PH_2CH_2SCH_3)_2]^{2+}$ (**5**) and $[Au_2(PH_2CH_2SCH_3)_2]^{2+}\cdot(MeCN)_2$ (**6**) complexes using the MP2 and CIS methods, respectively.

3.6. Head-to-Tail $[Au_2(PH_2CH_2SCH_3)_2]^{2+}$ and $[Au_2(PH_2CH_2SCH_3)_2]^{2+}\cdot(MeCN)_2$. The calculations on the head-to-tail $[Au_2(PH_2CH_2SCH_3)_2]^{2+}$ (**5**) and $[Au_2(PH_2CH_2SCH_3)_2]^{2+}\cdot(MeCN)_2$ (**6**) moieties were carried out to study the substituent effect on the sulfur atom of the complexes. The ground- and excited-state structures of **5** and **6** were fully optimized by the MP2 and CIS methods, respectively. The calculated geometry parameters are presented in Table 1, and the corresponding structures are depicted in Figure 5. As seen in Table 1, all the geometry parameters in the ^1A_g ground state of **5** agree with the corresponding X-ray diffraction data for $[Au_2(PPh_2CH_2SPh)_2]\cdot(CF_3SO_3)_2$.[25] Comparison between **1** and **5** as well as **2** and **6** in Table 1 indicated that the CH_3 substituent on the S atom in **5** and **6** affects very slightly the molecular geometry. Only the Au−S bond length is about 0.03 Å shorter and the Au−N distance elongates from 2.567 Å of **2** to 2.898 Å of **6** in the ^1A_g ground state. The enhancement of the donor ability of the sulfur atom by the electron donating CH_3 group in **5** and **6** strengthens the S→Au bonding, thus in the competition among P→Au, S→Au, and N···Au, the N···Au interaction is naturally weakened.

The CIS calculations showed that the ^3A_u excited states of **5** and **6** give rise to the lowest-energy 333 and 585 nm phosphorescent emissions with the $^3A_u \rightarrow {}^1A_g$ transition, respectively corresponding to the cases in the gas phase and solution. The natural atomic orbital populations of the ^3A_u excited state and the ^1A_g ground state as shown in S-Table 3 (Supporting Information) indicated that both the emissions originate from the MC transitions, which are consistent with the 337 nm emission of **1** and the 614 nm emission of **2**. Such calculated results revealed that the CH_3 group on the S atom in **5** and **6** causes the blue shift of the emission wave-

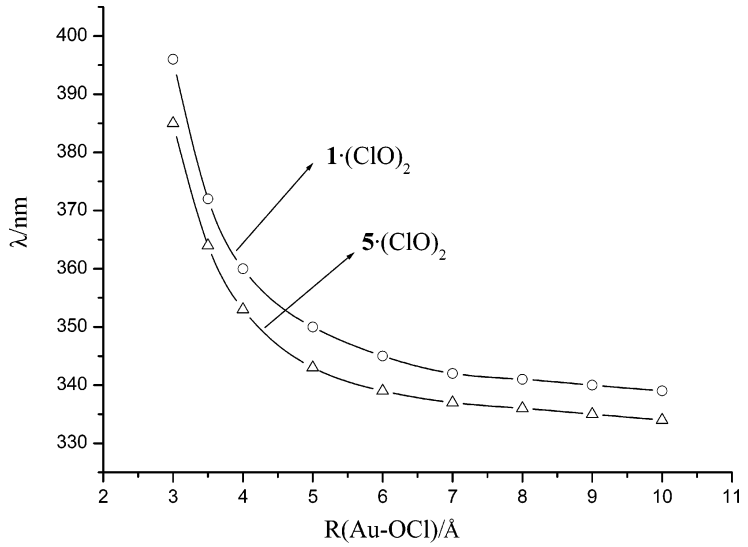

Figure 6. Plot of emission wavelength versus R(Au−OCl) (distance between Au atom and ClO^- anion) for $[Au_2(PH_2CH_2SH)_2]\cdot(ClO)_2$ [**1**·$(ClO)_2$] and $[Au_2(PH_2CH_2SCH_3)_2]\cdot(ClO)_2$ [**5**·$(ClO)_2$].

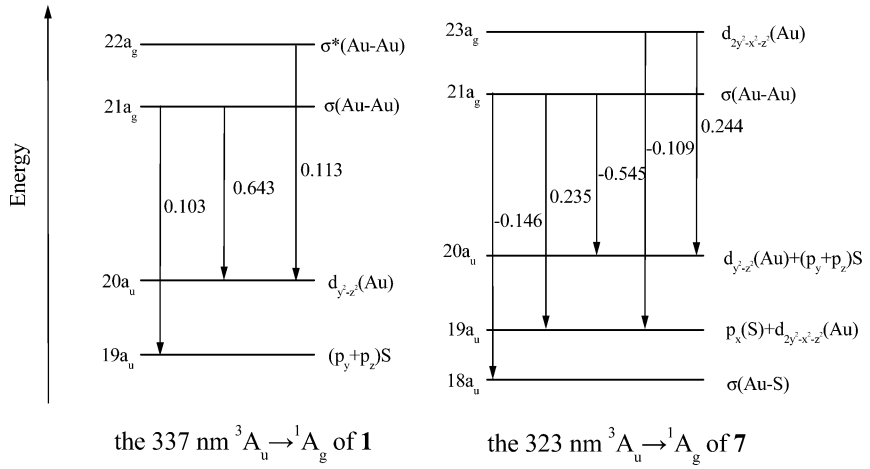

Figure 7. The diagrams of the single electron transition involved in the CIS wave function with |CI coefficient| > 0.1 for the lowest-energy emissions of $[Au_2(PH_2CH_2SH)_2]^{2+}$ (**1**) and $[Au_2(PH_2CH_2S)]$ (**7**).

length with respect to **1** and **2**. In **5** and **6**, the stronger donor ability of the S atom caused by the CH_3 group increases the Au−S σ bonding contribution to the lowest-energy emission. Besides two dominant CI configurations of **2** as shown in Figure 4, the $34a_u \rightarrow 36a_g$ configuration (CI coefficient of about 0.136) is involved in the 585 nm emission for **6** as illustrated in S-Figure III (Supporting Information). The $34a_u$ orbital has the Au−S σ bonding character, and the $34a_u \rightarrow 36a_g$ configuration increases the energy gap between the ^3A_u and ^1A_g states.

5·$(ClO)_2$ was applied to simulate the solid-state behavior of **5**, just as the model of **1**·$(ClO)_2$ used above. When the R(Au−OCl) distance changes from 10 to 3 Å, the corresponding emission varies from 334 to 385 nm. Figure 6 clearly reflects the correlation between the emission wavelength and R(Au−OCl) for **1**·$(ClO)_2$ and **5**·$(ClO)_2$, in which the substituent CH_3 group on the S atom for **5**·$(ClO)_2$ makes the emission wavelength blue-shift with respect to **1**·$(ClO)_2$ along with the whole curves.

3.7. The Comparison between the Au(I) Thioether and Thiolate Complexes. The above discussions indicated that the Au(I) thioether complexes with the S→Au dative bonding give rise to luminescence with the MC transitions either in the solid state or in solution. Very recently, we carried out the calculations on the head-to-tail Au(I) thiolate $[Au_2(PH_2CH_2S)_2]$ (**7**) with the S−Au covalent bonding to investigate its electronic structures of the ground state and the excited state.[36] The comparison between the Au(I) thioether and Au(I) thiolate complexes can provide insight into different roles played by the S→Au dative and S−Au covalent bondings in both electronic structures and transition properties.

Usually, the S−Au covalent bond is stronger and shorter than the S→Au dative bond, which is clearly presented by the comparison of optimized geometry parameters between **1** (thioether complex) and **7** (thiolate complex) in both the ^1A_g and ^3A_u states as listed in Table 1 and S-Table 4 (Supporting Information). The distances between S and Au in **7** are 0.07 Å and 0.24 Å shorter than those in **1** for the ^1A_g and the ^3A_u states, respectively.

(36) Pan, Q.-J.; Zhang, H.-X. *J. Chem. Phys.* **2003**, *119*, 4346.

Figure 7 presents the diagrams of the single electron transition with |CI coefficient| > 0.1 in the CIS calculations for the 337 and 323 nm $^3A_u \rightarrow {}^1A_g$ emissions of **1** and **7**, respectively. Of the three electron excitations involved in the $^3A_u \rightarrow {}^1A_g$ emission of **1**, the $21a_g \rightarrow 20a_u$ (coefficient = 0.643) and $22a_g \rightarrow 20a_u$ (coefficient = 0.113) configurations have pure MC transition character, while the $21a_g \rightarrow 19a_u$ configuration with only coefficient = 0.103 is the MMLCT transition. In the $^3A_u \rightarrow {}^1A_g$ emission of **7**, all the electron excitations are clearly mixed by the MMLCT and MC transitions. Therefore, the S→Au dative bond results in MC transition, but the S−Au covalent bond causes the mixture of the MMLCT and MC transitions. This difference in transition between the S→Au and S−Au bonds can also be interpreted by the density diagrams of the $^3A_u \rightarrow {}^1A_g$ emissions of **1** and **7** as shown in S-Figures V and VI (Supporting Information) that we do not discuss in detail here. Apparently, in Au(I) thiolate complexes, the thiolate ligand is greatly involved in the emissive process, but it is not the case for the Au(I) thioether.

4. Summary

The ab initio calculations on the title complexes indicate that Au^I-Au^I aurophilicity exists in the ground state and is strongly strengthened in the excited state, because the promotion of electrons from the antibonding d_{σ^*} (HOMO) to the bonding s_σ and/or p_σ (LUMO) results in the formation of an Au−Au σ single bond between two Au(I) atoms in the excited state. The aurophilicity can stabilize the excited state of **1**, which causes a large red shift in emission wavelength relative to the **8** monomer. The solvent effect strongly affects the luminescence of the phosphinothioether Au(I) complexes, and the red shift was found in **2** (614 nm) corresponding to **1** (337 nm). The coordination from acetonitrile to Au(I) enhances the Au^I-Au^I aurophilicity, which is responsible for the red shift of phosphorescence in the ^3A_u excited state in solution. The studies on **5** and **6** with the CH_3 substituent on the S atom indicate that the CH_3 group on the S atom for the Au(I) complexes causes the blue shift of emission wavelength with respect to **1** and **2**. By comparison of **1** (thioether complex) and **7** (thiolate complex), it is concluded that the thiolate ligand is greatly involved in the emissive processes, but the thioether ligand does not participate in a similar charge transfer in the transitions.

Acknowledgment. This work is supported by the National Natural Science Foundation of China (No. 20173021).

Supporting Information Available: Figures depicting optimized structures for **3**−**7** and single electron transitions for **1**, **4**, **6**, and **7**. Tables of phosphorescence wavelengths and natural atomic orbital populations for **3**−**7** and optimized main geometry parameters for **7**. This material is available free of charge via the Internet at http://pubs.acs.org.

IC0300159